# Multi-Aperture Phased Arrays Versus Multi-beam Lens Arrays for mmW Multiuser MIMO

Akbar M. Sayeed
University of Wisconsin-Madison
akbar@engr.wisc.edu

***Abstract*—Multi-beamforming and data multiplexing is a key functionality for realizing the spatial multiplexing gains in multiuser MIMO systems at millimeter-wave (mmW) frequencies. Due to prohibitive complexity of conventional digital beamforming, two main approaches to hybrid analog-digital beamforming are being investigated that use either phased arrays or lens arrays for analog beamforming. While the two approaches are equivalent from a purely communication-theoretic perspective, they offer very different tradeoffs in terms of performance, complexity and power consumption. In particular, all existing phased array-based prototypes are limited to a single beam per aperture, due to hardware constraints, thereby necessitating the use of multiple smaller sub-arrays for multi-beam operation. On the other hand, the beam switching network presents a hardware challenge in lens array-based systems, thereby limiting the coverage achieved by particular radio-frequency chain. In this paper, we apply the beamspace MIMO framework to compare the achievable sum-rates in a small cell served by an access point using a lens array-based or phased array-based architecture. We also discuss the hardware complexity of the two architectures to enable performance-complexity-energy optimization.**

## I. Introduction

Millimeter-wave (mmW) wireless is emerging as a key technology for achieving multi-Gigabits/s (Gbps) rates and millisecond latency requirements as part of the vision for 5G cellular and beyond [1]–[4]. There are two key characteristics of mmW frequencies (30 GHz-300 GHz) that make them attractive for high-rate and low-latency use cases: i) large bandwidth (on the order of 1 GHz or more), and ii) highly-directional, quasi-optical communication through high gain narrow beams due to the small wavelength. As a result, dynamic beamspace MIMO – multiplexing data simultaneously over multiple beams with changing directions – is a key operational functionality for achieving high spatial reuse and spectral efficiency.

Transceiver architectures for multi-beamforming and tracking are thus critical for realizing beamspace MIMO in practice. The number of transmit/receive (T/R) mmW chains – each consisting of a mixer, amplifier, filter and data convertor – is a key measure of transceiver complexity and cost. Conventional digital beamforming is limited to arrays with a small number of antennas due to the requirement of a T/R chain for each antenna. [4]. Hybrid beamforming architectures that combine analog mmW beamforming with low-dimensional digital processing are attractive for high-dimensional array needed at access points (APs) [4]. There are two main hybrid beamforming architectures, as illustrated in Fig. 1. The widely known phased array-based architecture, in Fig. 1(a), uses a network of mmW phase shifters for beamforming. However, due to the high complexity of the phase shifter network for multiple beams, all existing phased array-based prototype systems are limited to single-beam phased arrays - multiple phased sub-arrays are needed for generating multiple beams. Fig. 1(b) illustrates another promising hybrid beamforming architecture - first proposed in [5] and called continuous aperture phased (CAP)-MIMO - that uses a lens array for beamforming [5], [6]. In this architecture, a mmW lens is used for spatial focusing and an antenna array on its focal surface is used for transmittin and receiving beams from different directions. It can be shown using the beamspace MIMO framework that a lens array approximates a spatial discrete Fourier transform inherent to beamforming, and an appropriately designed lens array can generate approximately orthogonal beams that span the entire spatial coverage area [5], [6]. Significantly, a lens array is not limited to a single beam – multiple beams can be simultaneously generated using a mmW beam selector network as shown in Fig. 1(b).

Lens arrays and phased arrays offer different tradeoffs in terms of performance, complexity, and energy efficiency [4]. However, this work is still not complete and new results continue to be reported [7], [8], [8]–[10]. In this paper, we investigate the design and performance analysis of phased arrays and lens arrays from the viewpoint of an AP serving multiple single-antenna mobiles stations (MSs) in a small cell [11], [12]. Our approach is based on the beamspace MIMO framework [4]–[6], [13], [14] that is naturally relevant to mmW MIMO systems. In Sec. II we discuss the basic parameters for describing an AP, equipped with a 2D antenna array, serving multiple users in a small-cell. In Sec. III, we discuss the optimum design of a phased array AP – consisting of multiple sub-arrays for generating multiple beams – from a per-user rate perspective. This optimum design naturally leads to the optimum number of beams or T/R chains for the phased array AP. In Sec. IV, we discuss the design of a CAP-MIMO AP using a lens array with the same number of T/R chains and the same total array size as the optimum phased array AP. Sec. V discusses dimension/complexity reduction at the AP using the concept of dominant beam selection [6], [15], and considers two linear processing receivers, the matched filter (MF) or maximal ratio combiner, and the minimum

This work was partly supported by the US National Science Foundation under grants 1548996, 1703389 and 1629713.

mean squared error (MMSE) receiver. Expressions for the sum-rates of the two AP transceivers are developed, including idealized (interference-free) expressions for per-user rate as a benchmark. Sec. VI presents numerical results illustrating the design and analysis framework outlined in this paper. The results indicate that the lens array-based CAP-MIMO AP can deliver significant performance gains over the phased-array transceiver, and offers a flexible platform for near-optimal performance-complexity optimization.

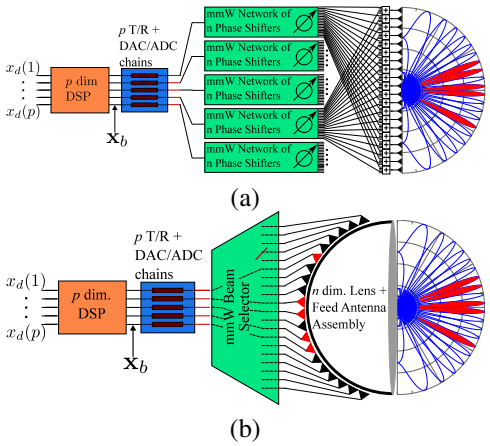


Fig. 1. (a) A multi-beam phased array transceiver. (b) A multi-beam CAP-MIMO transceiver with a lens array.

## II. Basic Small Cell and Access Point Parameters

Consider an AP with a 2D antenna of size $L = L_a \times L_e$, where $a$ and $e$ represent azimuth and elevation, respectively. The antenna dimension is given by

$$n = n_a \times n_e \ ; \ n_a = \frac{2L_a}{\lambda} \ , \ n_e = \frac{2L_e}{\lambda} \tag{1}$$

and $\lambda$ is the wavelength of operation. The array gain is given by [6]

$$G = n$$

and the array can generate $n$ orthogonal beams over the hemisphere. However, a smaller number of beams lie within the coverage area. Let $\phi_{e,max} \in (0, \pi/2]$ and $\phi_{a,max} \in (0, \pi/2]$ represent the maximum *one-sided* angular spreads for the coverage area in elevation and azimuth, as illustrated in Fig. 2. The number of orthogonal beams *within the coverage area* is given by

$$\begin{aligned} n_b = n_{b,a} \times n_{b,e} &= \frac{2\theta_{a,max}}{\Delta\theta_a} \times \frac{2\theta_{e,max}}{\Delta\theta_e} \\ &= n_a 2\theta_{a,max} \times n_e 2\theta_{e,max} \\ &= n_a \sin(\phi_{a,max}) \times n_e \sin(\phi_{e,max}) \\ &= n \sin(\phi_{e,max}) \sin(\phi_{a,max}) \end{aligned} \tag{2}$$

$$n_{b,a} = n_a \sin(\phi_{a,max}) \ , \ n_{b,e} = n_e \sin(\phi_{e,max}) \tag{3}$$

$$\text{where } \Delta\theta_e = \frac{1}{n_e} \text{ and } \Delta\theta_a = \frac{1}{n_a} \tag{4}$$

are the spacings between orthogonal beams which also represent the array resolution in azimuth and elevation.

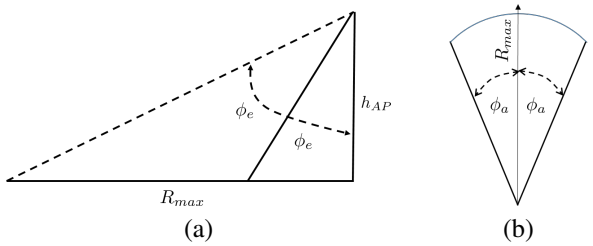


Fig. 2. (a) Elevation angular spread for a small cell of radius $R_{max}$ served by an AP at a height of $h_{AP}$. The AP array is pointed so that the broadside direction bisects the elevation and azimuth angular spreads. (b) Azimuth angular spread for the coverage area.

### A. Sector Angular Spreads

How are $\phi_{e,max}$ and $\phi_{a,max}$ determined? Basically, $\phi_{a,max}$ is determined by the (two-sided) sector angular spread in azimuth as illustrated in Fig. 2(b). For example for a 120 degree two-sided sector in azimuth, $\phi_{a,max} = \pi/3$ (60 degrees). The elevation angular spread is determined by the height of AP, $h_{AP}$, relative to the maximum cell radius $R_{max}$ as illustrated in Fig. 2(a):

$$\phi_{e,max} = \frac{1}{2} \tan^{-1}\left(\frac{R_{max}}{h_{AP}}\right) \text{ (one-sided)} \tag{5}$$

where we have assumed that the AP array is oriented so that its broadside direction bisects the angular spreads in elevation and azimuth as illustrated in Fig. 2.

### B. AP Antenna Size and Aspect Ratio

One of the first questions is: what is the size of the AP antenna array? The array size $n$ determines the array gain and the number of orthogonal beams, and it choice depends on the SNR requirements, cell size, the number of users $K$, and the number of RF chains. From a system perspective, a useful constraint is that the total number of orthogonal beams $n_b$ within the coverage area is related to the number of users $K$; ideally $n_b \geq K$ to exploit multiplexing gain. At the very least, $n_b$ should be bigger than the number of RF chains. Thus, we have

$$n_b \geq N_{RF} \text{ or } n_b \geq K \tag{6}$$

Regardless of how we choose $n_b$, knowing the angular spreads, we can determine the size of antenna array using (2) as

$$n = \frac{n_b}{\sin(\phi_{a,max}) \sin(\phi_{e,max})} \ , \ L = \frac{n\lambda}{2} \ . \tag{7}$$

Once we know $n$ (or $L$), the next question is how do we choose $n_a$ and $n_e$ (or $L_a$ and $L_e$)? This essentially determines the aspect ratio of the antenna array:

$$\alpha = \frac{n_a}{n_e} \ . \tag{8}$$

There are three main possibilities.

**Case I:** Equal number of orthogonal beams in the azimuth and elevation angular spreads; that is, $n_{b,a} = n_{b,e} = \sqrt{n_b}$

$$\alpha = \frac{n_a}{n_e} = \frac{\sin(\phi_{e,max})}{\sin(\phi_{a,max})} \tag{9}$$

$$n_a = \frac{\sqrt{n_b}}{\sin(\phi_{a,max})} \ , \ n_e = \frac{\sqrt{n_b}}{\sin(\phi_{e,max})} \tag{10}$$

$$n_{b,a} = n_{b,e} = \sqrt{n_b} \tag{11}$$

**Case II:** Equal number of antennas in azimuth and elevation; that is, $n_a = n_e = \sqrt{n}$

$$\alpha = \frac{n_a}{n_e} = 1 \tag{12}$$

$$n_a = n_e = \sqrt{n} = \sqrt{\frac{n_b}{\sin(\phi_{a,max})\sin(\phi_{e,max})}} \tag{13}$$

$$n_{b,a} = \sqrt{\frac{n_b \sin(\phi_{a,max})}{\sin(\phi_{e,max})}} \ , \ n_{b,e} = \sqrt{\frac{n_b \sin(\phi_{e,max})}{\sin(\phi_{a,max})}} \tag{14}$$

**Case III:** The number of antennas azimuth/elevation is proportional to the corresponding angular spreads:

$$\alpha = \frac{n_a}{n_e} = \frac{\sin(\phi_{a,max})}{\sin(\phi_{e,max})} \tag{15}$$

$$n_a = \frac{\sqrt{n_b}}{\sin(\phi_{e,max})} \ , \ n_e = \frac{\sqrt{n_b}}{\sin(\phi_{a,max})} \tag{16}$$

$$n_{b,a} = \frac{\sqrt{n_b}\sin(\phi_{a,max})}{\sin(\phi_{e,max})} \ , \ n_{b,e} = \frac{\sqrt{n_b}\sin(\phi_{e,max})}{\sin(\phi_{a,max})} \tag{17}$$

We will primarily consider Case I in this paper.

### C. User Coordinates

We now describe user coordinates within the 3D geometry of the small cell illustrated in Fig. 2. The base of the AP is at the origin $(x, y, z) = (0, 0, 0)$ with the location of AP given by $(x, y, z) = (0, 0, h_{AP})$. The users are located in the $x - y$ plane and the $y - z$ plane contains the broadside direction for the AP array. The user coordinates are uniquely determined by specifying any one of the following pairs of variables:

$$(x, y) \Longleftrightarrow (\phi_a, \phi_e) \Longleftrightarrow (R, \phi_a) \tag{18}$$

where $R$ is the distance of the user from the base of the AP (origin). For given angular directions $(\phi_a, \phi_e) \in [-\phi_{a,max}, \phi_{a,max}] \times [-\phi_{e,max}, \phi_{e,max}]$ for a user, its $(x, y)$ coordinates and distance $R$ from the AP are given by

$$R = h_{AP}\tan(\phi_e + \phi_{e,max}) \ , \ R_{AP} = \sqrt{R^2 + h_{AP}^2}$$
$$x = R\sin(\phi_a) \ , \ y = R\cos(\phi_a) \tag{19}$$

For a given $(R, \phi_a) \in [0, R_{max}] \times [-\phi_{a,max}, \phi_{a,max}]$, the $(x, y)$ coordinates and $R_{AP}$ are given as above with

$$\phi_e = \tan^{-1}\left(\frac{R}{h_{AP}}\right) - \phi_{e,max} \tag{20}$$

For a given $(x, y)$

$$R = \sqrt{x^2 + y^2} \ , \ \phi_a = \sin^{-1}\left(\frac{x}{R}\right) \tag{21}$$

and $\phi_e$ is determined via (20).

## III. Multi-Aperture Phased Array Optimization

In this section, we discuss the optimum design of an AP with a phased array transceiver. We assume that only a single beam can be generated from a single phased array, reflecting the state-of-the-art. Thus, in order to generate multiple simultaneous beams, multiple sub-arrays (multiple apertures) are needed. In order to compare lens arrays and phased arrays, we assume a fixed array size for both kinds of arrays.

### A. Array Partitioning

Consider a phased of dimension $n$ which is partitioned into $N_s = N_{s,a} \times N_{s,e}$ sub-arrays where $n = N_s n_s$ and $n_s$ is the dimension of each sub-array which can be factored as:

$$n_s = \frac{n}{N_s} = n_{s,a} \times n_{s,e} = \frac{n_a}{N_{s,a}} \times \frac{n_e}{N_{s,e}}$$
$$n_{s,a} = \frac{n_a}{N_{s,a}} \ ; \ n_{s,e} = \frac{n_e}{N_{s,e}} \tag{22}$$

The number of maximum number of orthogonal beams (within the coverage area) associated with each sub-array is given by

$$n_{b,s} = \frac{n_b}{N_s} = n_{b,sa} \times n_{b,se}$$
$$n_{b,sa} = n_{s,a}\sin(\phi_{a,max}) = \frac{n_a}{N_{s,a}}\sin(\phi_{a,max}) = \frac{n_{b,a}}{N_{s,a}}$$
$$n_{b,se} = n_{s,e}\sin(\phi_{e,max}) = \frac{n_e}{N_{s,e}}\sin(\phi_{e,max}) = \frac{n_{b,e}}{N_{s,e}} \tag{23}$$

### B. Optimum Partitioning

For optimum phased array design, a natural questions is: *For a given array dimension $n$, what is the optimum number of sub-arrays, $N_s$, and the corresponding dimension of each sub-array, $n_s$, that maximizes the small cell sum-rate (or average per-user rate)?*

The answer to this question depends on the SNR and is guided by two cases. First, consider the case when $N_s = 1$ and $n_s = n$. In this case, there is a single sub-array and hence only one beam. This results in no beamspace multiplexing but it gives the highest antenna gain. This configuration is optimum in the low SNR regime.

The second case is more interesting for which $1 < N_s < n$ and $1 < n_s < n$. In this case, we can have $N_s$ beams, with one beam associated with each sub-array. This is useful from the viewpoint of multiplexing gain as long as the SNR is sufficiently high. Thus, we want $N_s$ as large as possible in the high-SNR regime. However, even in the high-SNR regime, there is a limit to how large $N_s$ can be. This is due to the fact that each of the $N_s$ sub-arrays must be able to generate at least $N_s$ orthogonal (or sufficiently linearly independent) beams within the coverage area in order for the full array to achieve an $N_s$-fold multiplexing gain; that is, $n_{b,s} \geq N_s$. However, recall that $n_{b,s} = n_b/N_s$. Thus, we have

$$N_s \leq \sqrt{n_b} \Longleftrightarrow N_{s,a} \times N_{s,e} \leq \sqrt{n_{b,a}} \times \sqrt{n_{b,e}}$$

and for sufficiently high SNR, the optimum (largest) value of $N_s$ is given by

$$N_{s,opt} = \sqrt{n_b} \tag{24}$$

$$\Updownarrow$$

$$N_{s,a,opt} = \sqrt{n_{b,a}} = \sqrt{n_a \sin(\phi_{a,max})}$$

$$N_{s,e,opt} = \sqrt{n_{b,e}} = \sqrt{n_e \sin(\phi_{e,max})} \tag{25}$$

For the above optimum array partitioning, we have the following dimensions for each sub-array

$$n_{s,opt} = \frac{n}{N_{s,opt}} = \frac{n}{\sqrt{n_b}} = \frac{\sqrt{n_b}}{\sin(\phi_{a,max})\sin(\phi_{e,max})}$$
$$= n_{s,a,opt} \times n_{s,e,opt} \tag{26}$$

$$n_{s,a,opt} = \frac{n_a}{N_{s,a,opt}} = \frac{n_a}{\sqrt{n_{b,a}}} = \sqrt{\frac{n_a}{\sin(\phi_{a,max})}} \tag{27}$$

$$n_{s,e,opt} = \frac{n_e}{N_{s,e,opt}} = \frac{n_e}{\sqrt{n_{b,e}}} = \sqrt{\frac{n_e}{\sin(\phi_{e,max})}} \tag{28}$$

In terms of the beams generated by each sub-array, we have

$$n_{b,s,opt} = \frac{n_b}{N_{s,opt}} = \sqrt{n_b} = N_{s,opt}$$
$$= \sqrt{n_{b,sa,opt}} \times \sqrt{n_{b,se,opt}} \tag{29}$$

$$n_{b,sa,opt} = \frac{n_{b,a}}{N_{s,a,opt}} = \frac{n_{b,a}}{\sqrt{n_{b,a}}} = N_{s,a,opt}$$
$$= \sqrt{n_a \sin(\phi_{a,max})} \tag{30}$$

$$n_{b,se,opt} = \frac{n_{b,e}}{N_{s,e,opt}} = \frac{n_{b,e}}{\sqrt{n_{b,e}}} = N_{s,e,opt}$$
$$= \sqrt{n_e \sin(\phi_{e,max})} \tag{31}$$

Recall that an AP with an $N_s$-aperture phased array can generate $N_s$ simultaneous beams, each driven by one of the $N_{RF} = N_s$ RF chains. For $K$ users to serve in the coverage area, the number of users per RF chain/beam is given by

$$K_{RF} = \frac{K}{N_s} = \frac{K}{\sqrt{n_b}}$$

where the last equality is for the optimum design. Thus, the total bandwidth $W$ is shared by $K_{RF}$ users on average in each beam. The idealized (interference-free) per-user uplink rate (bps) at a distance $R$ is given by

$$C_{PA}(R) = \frac{W}{K_{RF}} \log_2\left(1 + \frac{PG_s\gamma}{N_o W/K_{RF}}\right), \ \gamma = \left(\frac{\lambda}{4\pi R}\right)^2$$

where $\gamma$ is the free-space pathloss, $G_s = n_s$ is the array gain for each sub-array, $N_o = kT$ is the noise power spectral density[1], and $P$ is the per-user transmitted power. The average per-user rate for a phased array AP is illustrated in Fig. 3 for different values of $1 \le N_s \le \sqrt{n_b}$. For every SNR there is an optimum $N_s$ and for high SNR $N_s = \sqrt{n_b}$ is optimal. This is related to results on reconfigurable antenna arrays in [16].

[1] $k = 1.38 \times 10^{-23}$ is the Boltzmann constant, and $T$ is the operating temperature in degrees Kelvin ($T = 300$K at room temperature).

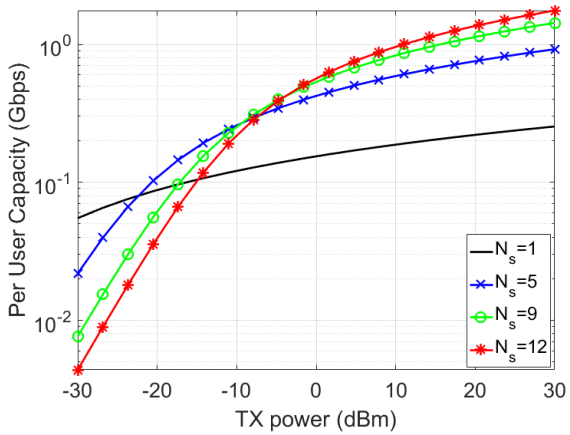


Fig. 3. The ideal per-user rate for a phased array AP for different number of sub-arrays $N_s$ for $n = 240$ and $n_b = 144$.

## IV. Multi-Beam CAP-MIMO Optimization

Suppose that we have chosen the optimum antenna dimension $n$, the beams over the coverage area $n_b$, the antenna aspect ratio $\alpha$ and the optimum phased array AP configuration. The number of sub-arrays in the optimum phased array configuration determines the number of RF chains: $N_{RF} = N_{s,opt} = \sqrt{n_b}$. For comparison with CAP-MIMO, a natural question is: *Given an array size $n$ and the optimum phased array AP configuration, what is the optimum CAP-MIMO configuration for the same number of RF chains, $N_{RF} = \sqrt{n_b}$, that maximizes the sum-rate (or average per-user rate)?*

An obvious choice is to use the full aperture for each beam so that we have the highest antenna gain. So, we choose a single aperture of maximum dimension $n$ and maximum number of orthogonal beams $n_b$ within the coverage area. How do we allocate the RF chains? The simplest solution is to partition the coverage area into $N_{sec} = N_{RF} = \sqrt{n_b}$ sectors and associate each sector with one RF chain. Let us assume uniform-sized sectors for simplicity. The number of orthogonal (high-resolution) beams per sector is given by

$$n_{b,sec} = \frac{n_b}{N_{sec}} = \sqrt{n_b} \tag{32}$$

which is identical to the number of orthogonal beams, $n_{b,s,opt}$, generated by each sub-array in an optimized phased array AP (to span the entire coverage area). In this case, each RF chain for each sector can be mapped to one of the $n_{b,sec}$ beams through a $1 \mapsto n_{b,sec}$ switch.

We can reduce the switch complexity if the maximum number of expected users is $K$. A good extreme design choice is to have a total of $n_{b,2} = K$ (broader) orthogonal beams over the coverage area and

$$n_{b,sec,2} = \frac{n_{b,2}}{N_{sec}} = \frac{K}{\sqrt{n_b}} \ (= K_{RF}) \tag{33}$$

(broader) orthogonal beams in each disjoint sector. This requires a $1 \mapsto n_{b,sec,2}$ switch in each beamspace sector,

which would be of lower complexity as long as $K \leq n_b$, which would typically be the case for the high-resolution beams; see (6). Note that, in this case, the feed antennas will have to designed appropriately to generate broader beams. In general, the size/area of the feed antenna is proportional to the beamwidth. The number of (high resolution) orthogonal beams within the broader beam is given by

$$n_{b,f} = \frac{n_{b,sec}}{n_{b,sec,2}} = \frac{n_b}{K} \tag{34}$$

and thus the new composite feed antennas would cover the area of about $n_{b,f}$ (highest resolution) feed antennas to generates a correspondingly wide beam to avoid holes in coverage.

In general, for a given number of users $K$ and the antenna size $n$ (or equivalently $n_b$), we have a whole family of choices for the switch dimension (SD)

$$\frac{K}{\sqrt{n_b}} \leq \text{SD} \leq \sqrt{n_b} \tag{35}$$

with the corresponding composite feed size (relative to the high-resolution feed size) given by

$$1 \leq n_{b,f} = \frac{n_{b,sec}}{SD} \leq \frac{n_b}{K} \tag{36}$$

which ranges between $n_{b,f} = 1$ (for the largest $SD = \sqrt{n_b}$) and $n_{b,f} = \frac{n_b}{K}$ (for the smallest $SD = \frac{K}{\sqrt{n_b}}$). The number of beams in azimuth and elevation in a composite feed are related through the choice of the antenna aspect ratio $\alpha$ as discussed in Sec. II-B. For equal beams in the azimuth and elevation directions (Case I), we have

$$n_{b,fa} = n_{b,fe} = \sqrt{n_{b,f}} \ .$$

The idea of a composite is also attractive from the viewpoint of maximizing the power transfer from the feed to the lens. It can be shown that, in order to get the best coupling to the aperture, the feed size needs to be a bit larger than that specified by the critical spacing.

For a given number of RF chains, there are other possibilities as well for CAP-MIMO. For example, multiple apertures may be more attractive from an implementation viewpoint. However, multiple apertures will usually result in a loss of SNR. But it will still be less than that in a phased array system as long as the number of apertures used in CAP-MIMO is less that in the phased array system.

One interesting possibility of multiple apertures in CAP-MIMO is related to the feed complexity. For a given $n_{b,f} > 1$, typically a composite feed with an area of about $n_{b,f}$ critically-spaced (high resolution) feeds would be needed for generating a broader beam. However, an alternative is to use $n_{b,f}$ apertures, with each aperture of a smaller size by a factor of $n_{b,f}$ compared to the maximum aperture size, resulting in correspondingly larger beams. In this case, we can use regular, single-beam (high-resolution) feeds. The signal for each (broader) beam is now generated coherently by multiple apertures, and the combined signal would compensate for the SNR loss due to smaller apertures/wider beams from each aperture. However, the wider beams will result in higher interference.

## V. System Model and Beamspace Processing at AP

Consider a small cell in which an AP with a 2D uniform planar array of dimension $n = n_a \times n_e$ serves $K$ users in a sector of radius $R_{max}$ and angular spreads $\phi_{a,max}$ and $\phi_{e,max}$. We consider uplink operation. The received signal at the AP is given by

$$\boldsymbol{r} = \sum_{k=1}^{K} \boldsymbol{h}_k \beta_k s_k + \boldsymbol{w} = \boldsymbol{H}\boldsymbol{\beta}\boldsymbol{s} + \boldsymbol{w} \ , \ \boldsymbol{H} = [\boldsymbol{h}_1, \cdots, \boldsymbol{h}_K]$$
$$\boldsymbol{\beta} = \text{diag}(\beta_1, \cdots, \beta_K) \ , \ \boldsymbol{s} = [s_1, \cdots, s_K]^T \tag{37}$$

where $\boldsymbol{w} \sim \mathcal{N}(\boldsymbol{0}, N_o \boldsymbol{I}_n)$ is the $n \times 1$ complex AWGN noise vector with power spectral density $N_o$, and $s_k$ is the transmitted signal, $\beta_k$ the complex path loss, and $\boldsymbol{h}_k$ the $n \times 1$ channel vector for user $k$:

$$\beta_k = e^{j\psi_k} \frac{\lambda}{4\pi R_k} \ , \ \boldsymbol{h}_k = \boldsymbol{a}_n(\theta_k) \ , \ \theta_k = (\theta_{a,k}, \theta_{e,k}) \tag{38}$$

In (38), $R_k$ is the distance from the AP, and $\boldsymbol{a}_n(\theta_k)$ is the $n \times 1$ the array response (column) vector in the direction $\theta_k = (\theta_{a,k}, \theta_{e,k})$, relative to broadside of AP, of user $k$:

$$\boldsymbol{a}_n(\theta) = \boldsymbol{a}_n((\theta_a, \theta_e)) = \boldsymbol{a}_{n_a}(\theta_a) \otimes \boldsymbol{a}_{n_e}(\theta_e) \tag{39}$$
$$\boldsymbol{a}_n(\theta) = \left[e^{-j2\pi\theta i}\right]_{i \in \mathcal{I}_n} \tag{40}$$
$$\mathcal{I}_n = \left\{ i - \frac{(n-1)}{2} : i = 0, \cdots, n-1 \right\} \tag{41}$$

where $\otimes$ denotes the kronecker product [17]. We assume that the transmitted signals of different users are independent with powers $\rho_k = E[|s_k|^2]$. The beamspace representation of $\boldsymbol{r}$ is given by [12]

$$\boldsymbol{r}_b = \boldsymbol{U}^H \boldsymbol{r} = \boldsymbol{H}_b \boldsymbol{\beta}\boldsymbol{s} + \boldsymbol{w}_b \ , \ \boldsymbol{H}_b = [\boldsymbol{h}_{b,1}, \cdots, \boldsymbol{h}_{b,K}] \tag{42}$$
$$\boldsymbol{h}_{b,k} = \boldsymbol{U}^H \boldsymbol{h}_k = \left[\boldsymbol{U}_{n_a}^H \boldsymbol{a}_{n_a}(\theta_{a,k})\right] \otimes \left[\boldsymbol{U}_{n_e}^H \boldsymbol{a}_{n_e}(\theta_{e,k})\right] \tag{43}$$

where $\boldsymbol{U} = \boldsymbol{U}_{n_a} \otimes \boldsymbol{U}_{n_e}$ is a 2D DFT matrix and

$$\boldsymbol{U}_n = \left[\frac{1}{\sqrt{n}} \boldsymbol{a}_n(\Delta\theta_n i)\right]_{i \in \mathcal{I}(n)} \ , \ \Delta\theta_n = \frac{1}{n} \tag{44}$$

denotes an $n \times n$ unitary DFT matrix whose columns are steering vectors in uniformly spaced directions $\theta_i = \Delta\theta_n i$ with spacing $\Delta\theta_n$, the spatial resolution of an $n$-dimensional array. The columns of $\boldsymbol{U}_n$ represent an orthonormal basis for the $n$-dimensional spatial signal space of the array. In (43), the component vectors of $\boldsymbol{h}_{b,k}$ (in azimuth and elevation)

$$\boldsymbol{U}_n^H \boldsymbol{a}_n(\theta) = \left[\frac{1}{\sqrt{n}} \frac{\sin(\pi n(\theta - i\Delta\theta_n))}{\sin(\pi\theta)}\right]_{i \in \mathcal{I}(n)} \tag{45}$$

are samples of a scaled Dirichlet sinc function with a maximum value of $\sqrt{n}$ reflecting the array gain.

### A. Dimension Reduction through Beam Selection

A key advantage of beamspace MIMO is that it enables transceiver complexity reduction by exploiting the sparsity of mmW channels in beamspace. The $N_{RF}$ available mmW transmit/receive chains are connected to $N_{RF}$ dominant beams carrying most of the multiuser signal power. One simple way

to select these dominant beams is to choose the beams with the largest aggregate power; that is, define the sparsity mask $\mathcal{M}$ as the set of indices of the $N_{RF}$ largest entries of the beamspace power vector

$$\boldsymbol{p}_b = \sum_{k=1}^{K} |\boldsymbol{h}_{b,k}|^2 \ ; \ p_b(i) = |h_{b,k}(i)|^2 \ , \ i = 1, \cdots, n_b \quad (46)$$

The AP selects the beams in $\mathcal{M}$ and connects them to the $N_{RF}$ chains and the corresponding $N_{RF}$ beams in (42) are then processed.[2] From now on, we refer to $\boldsymbol{r}_b$ as this $N_{RF}$-dimensional vector corresponding to an $N_{RF} \times K$ submatrix of $\boldsymbol{H}_b$ in (42).

### B. Linear Interference Suppression in Beamspace

We consider linear interference suppression schemes at the AP for both CAP-MIMO and phased array receivers represented by an $N_{RF} \times K$ matrix $\boldsymbol{L}_b = [\boldsymbol{\ell}_{b,1}, \cdots, \boldsymbol{\ell}_{b,K}]$ that operates on the selected $N_{RF}$ dominant beams:

$$\boldsymbol{z}_b = \boldsymbol{L}_b^H \boldsymbol{r}_b = \boldsymbol{L}_b^H \boldsymbol{H}_b \boldsymbol{\beta} \boldsymbol{s} + \boldsymbol{L}_b^H \boldsymbol{w}_b \quad (47)$$

where $\boldsymbol{L}_b^H \boldsymbol{w}_b \sim \mathcal{N}(\boldsymbol{0}, N_o \boldsymbol{L}_b^H \boldsymbol{L}_b)$. We consider two types of spatial filtering matrices $\boldsymbol{L}_b$

$$\boldsymbol{L}_{b,mf}^H = \boldsymbol{H}_b^H \quad (48)$$

$$\boldsymbol{L}_{b,mmse}^H = \boldsymbol{\Lambda}_s \boldsymbol{\beta}^H \boldsymbol{H}_b^H (\boldsymbol{H}_b \boldsymbol{\beta} \boldsymbol{\Lambda}_s \boldsymbol{\beta}^H \boldsymbol{H}_b^H + N_o \boldsymbol{I})^{-1} \quad (49)$$

where $\boldsymbol{L}_{b,mf}$ represents the matched filter (MF) receiver, $\boldsymbol{L}_{b,mmse}$ represents the minimum mean squared error (MMSE) receiver, and $\boldsymbol{\Lambda}_s = E[\boldsymbol{s}\boldsymbol{s}^H] = \mathrm{diag}(\rho_1, \cdots, \rho_K)$ is a diagonal matrix of transmit signal powers for the different users [14].

For a given $\boldsymbol{L}_b$, the spatially filtered signal for the $k$-th user is

$$\begin{aligned} z_{b,k} &= \boldsymbol{\ell}_{b,k}^H \boldsymbol{H}_b \boldsymbol{\beta} \boldsymbol{s} + \boldsymbol{\ell}_{b,k}^H \boldsymbol{w} \\ &= \boldsymbol{\ell}_{b,k}^H \boldsymbol{h}_{b,k} \beta_k s_k + \sum_{k'=1, k' \neq k}^{N_{RF}} \boldsymbol{\ell}_{b,k}^H \boldsymbol{h}_{b,k'} \beta_{k'} s_{k'} + \boldsymbol{\ell}_{b,k}^H \boldsymbol{w} \\ &= \mathrm{sig}_k + \mathrm{int}_k + \mathrm{noise}_k \end{aligned} \quad (50)$$

from which $\mathrm{SINR}_k$, the signal-to-interference-and-noise ratio for the $k$-th user, conditioned on a particular channel realization, can be calculated as

$$\begin{aligned} \mathrm{SINR}_k &= \frac{E[|\mathrm{sig}_k|^2]}{E[|\mathrm{int}_k|^2 + E[|\mathrm{noise}_k|^2]} \\ &= \frac{|\boldsymbol{\ell}_{b,k}^H \boldsymbol{h}_{b,k}|^2 |\beta_k|^2 \rho_k}{\sum_{k'=1, k' \neq k}^{N_{RF}} |\boldsymbol{\ell}_{b,k}^H \boldsymbol{h}_{b,k'}|^2 |\beta_{k'}|^2 \rho_{k'} + N_o \|\boldsymbol{\ell}_{b,k}\|^2} \end{aligned} \quad (51)$$

We note that the relations (50)-(51) correspond to a system with only $N_{RF}$ users (rather than $K$). It is based on the assumption of time-division multiplexing of the $K$ users through $N_{RF}$ RF chains/spatial channels. That is, in any given frame or time-slot, only $N_{RF}$ users are simultaneously served. All the $K$ users are served by selecting the dominant beams of different subsets of $N_{RF}$ users over different frames. A more detailed discussed of this "resource allocation" issue will be reported elsewhere.

[2]This beam selection assumes roughly comparable powers for each user. For other approaches to beam selection, see [11], [15].

### C. Sum-Rate and Average Per-User Rate

The ideal (interference-free) per-user rate is given by

$$C = W_u \log_2 \left(1 + \frac{PG\gamma}{N_o W_u}\right) \ \text{bits/s (bps)} \quad (52)$$

where $G$ is the array gain, $\gamma$ is the free-space path loss, $W_u$ is the per-user bandwidth and $K_{RF}$ is the number of users per RF chain:

$$K_{RF} = \frac{K}{N_{RF}} \ , \ W_u = \frac{W}{K_{RF}} = \frac{W N_{RF}}{K}$$

The main difference between the phased array and CAP-MIMO APs is in the array gain: $G = n$ for CAP-MIMO and $G_s = n/N_{RF}$ for phased array. Thus, the per-user rate for phased array and CAP-MIMO APs is given by

$$\begin{aligned} C_{PA}(R) &= \frac{W N_{RF}}{K} \log_2 \left(1 + \frac{PnK\gamma}{N_{RF}^2 N_o W}\right) \\ C_{CM}(R) &= \frac{W N_{RF}}{K} \log_2 \left(1 + \frac{PnK\gamma}{N_{RF} N_o W}\right) \end{aligned} \quad (53)$$

Accounting for interference, for a given $\boldsymbol{L}_b$, and treating the interference as Gaussian noise, it can be shown that the actual average per-user rate (bps) is given by [14]:

$$C(\boldsymbol{L}_b) = E_{\boldsymbol{H}_b}\left[\frac{W}{K_{RF}} \sum_{k=1}^{N_{RF}} \log_2 \left(1 + \mathrm{SINR}_k(\boldsymbol{L}_b, \boldsymbol{H}_b)\right)\right] \quad (54)$$

where $\mathrm{SINR}_k$ is defined in (51).

## VI. Numerical Results

In this section, we present some numerical results to illustrate the capacity comparison between phased array and CAP-MIMO APs in a small cell environment. The basic small cell parameters are: $R_{max} = 100$m $h_{AP} = 10$m, $\phi_{a,max} = 60^o$ and $\phi_{e,max} = 42^o$. The operating frequency and bandwidth are $f_c = 28$ GHz and $W = 1$ GHz, and $K = 100$ users.

We start with a given number of beams $n_b$ from which $n$, $n_a$ and $n_e$ can be determined by choosing a particular strategy for determining the array aspect ratio $\alpha$, as discussed in Sec. II-B. The optimum phased array and CAP-MIMO configurations can be determined as discussed in Sec. III and Sec. IV. In particular, for the optimum phased array configuration, we have

$$\begin{aligned} N_{s,opt} &= n_{b,s,opt} = \sqrt{n_b} = N_{RF} \\ n_{s,opt} &= \frac{n}{N_s} = \frac{\sqrt{n_b}}{\sin(\phi_{a,max}) \sin(\phi_{e,max})} \end{aligned} \quad (55)$$

Then we can determine the azimuth and elevation parameters as in Sec. III for the different aspect ratio cases. For Case I:

$$\begin{aligned} N_{sa,opt} &= N_{se,opt} = n_b^{1/4} \\ n_{sa,opt} &= \frac{n_b^{1/4}}{\sin(\phi_{a,max})} \ , \ n_{se,opt} = \frac{n_b^{1/4}}{\sin(\phi_{e,max})} \\ n_{b,sa,opt} &= n_{b,se,opt} = n_b^{1/4} \ . \end{aligned} \quad (56)$$

We illustrate our results by comparing the two types of APs for a scenario in which we span the coverage area with $n_b = 144$ beams, with $n_{b,e} = n_{b,a} = \sqrt{n_b} = 12$. This yields the antenna aperture size of $n = 240 = n_a \times n_e = 16 \times 15$, corresponding to $L_a = 3.4$" and $L_e = 3.2$". The optimum phased array and CAP-MIMO AP configurations, in the aperture and beamspace domains, are shown in Fig. 4. The optimum phased array configuration consists of 12 sub-

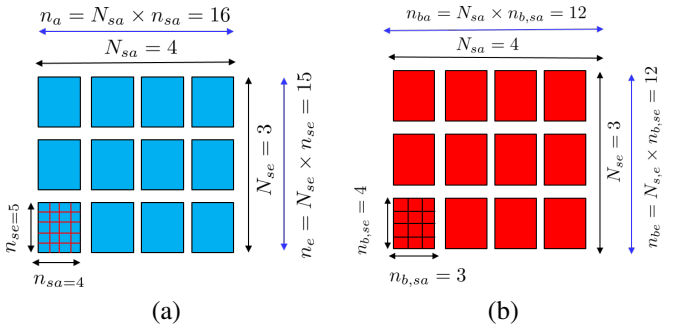


Fig. 4. Array configurations for $n_b = 144$ and $N_{RF} = \sqrt{n_b} = 12$ RF chains. (a) Optimal 12-aperture/12-beam phased array configuration. (b) CAP-MIMO configuration with 12 beamspace sectors, each sector consisting of 12 beams and driven by one RF chain.

arrays each of size $4 \times 5$ and driven by one RF chain. The CAP-MIMO configuration consists of 12 beamspace sectors, each with 12 beams and driven by an RF chain via a 1-to-12 switch. The switch dimension can be reduced by using multi-aperture or composite-feed CAP-MIMO configurations as discussed in Sec. IV. For example, composite feeds covering 2 high-resolution beams can be used to reduce the switch dimension from 12 to 6.

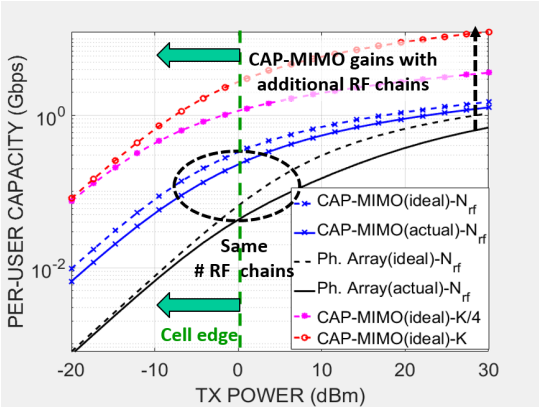


Fig. 5. Average per-user rate comparison of phased array and CAP-MIMO APs.

The comparison between phased array and CAP-MIMO APs in terms of per-user rate (in Gbps) as a function of transmit per-user power (in dBm) is shown in Fig. 5. The dashed lines represent the idealized rates from (53) for $N_{RF} = 12$. As evident, for the same number of RF chains, the CAP-MIMO AP achieves a nearly 10dB gain in SNR due to the higher array gain. However, unlike the phased array AP, the CAP-MIMO AP can readily incorporate more RF chains to generate a larger number of simultaneous beams, thereby increasing the per-user bandwidth $W_u$. Two idealized plots for CAP-MIMO AP rate for $N_{RF} = K/4$ and $N_{RF} = K$ are shown. As evident, CAP-MIMO can achieve a 3 to 10 fold increase in per-user rate by increasing $N_{RF}$.

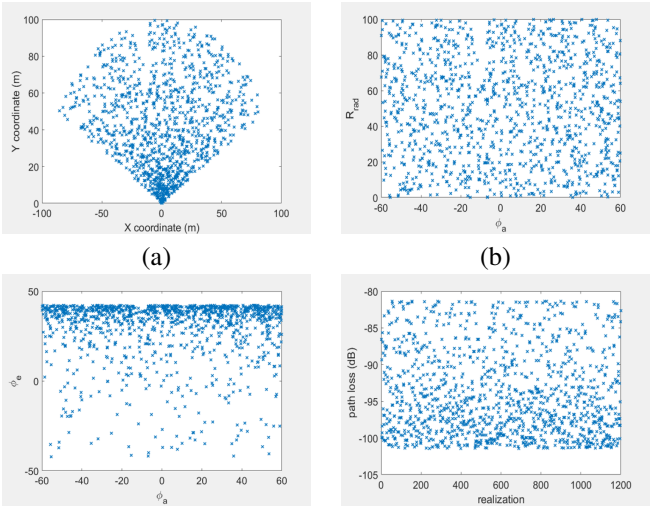


Fig. 6. Illustration of user LoS path parameters in the simulations. (a) the $(x, y)$ coordinates of the user locations in the coverage area. (b) The user location coordinates in $(R_{rad}, \phi_a)$. (c) The user location coordination in $(\phi_a,\phi_e)$. (d) Path loss of the user LoS paths as a function of the user location realization index.

Next we compare the actual performance of the two APs with interference suppression. For each realization, we generate the location of $N_{RF}$ users in the coverage area. The locations are based on randomly drawing user coordinates $(R_{rad}, \phi_a) \in [0, R_{max}] \times [-\phi_{a,max}, \phi_{a,max}]$. Figs. 6(a)-(c) show the locations of randomly chosen user coordinates in $(x, y)$, $(R_{rad}, \phi_a)$, and $(\phi_a, \phi_e)$. Fig. 6(d) shows the path loss for different user location realizations.

Returning back to Fig. 5, the solid line plots show the actual performance of the CAP-MIMO and phased array APs for the same number of RF chains, $N_{RF} = 12$, using the MMSE receiver for interference suppression. It is clear that the performance with interference suppression closely tracks the idealized performance, especially for the CAP-MIMO AP.

The beamspace representations of the channels seen by the phased array AP and the CAP-MIMO AP are illustrated in Fig. 7. The beamspace channel matrices $\boldsymbol{H}_b$ defined in (42) and (43), corresponding to kronecker-product beamspace channel vectors $\boldsymbol{h}_{b,k}$ for $N_{RF} = 12$ users, are shown in Figs.7(a)-(b). The corresponding channel matrices in azimuth and elevation orthogonal beam directions for one of the users are shown in Fig. 7(c)-(d). (Essentially reshaping one column of the kronecker matrices in Fig. 7(a)-(b) into a elevation-azimuth matrix.) The narrower beamwidth of the CAP-MIMO AP compared to the phased array AP is evident.

In fact, it can be shown that the beam area (product of the

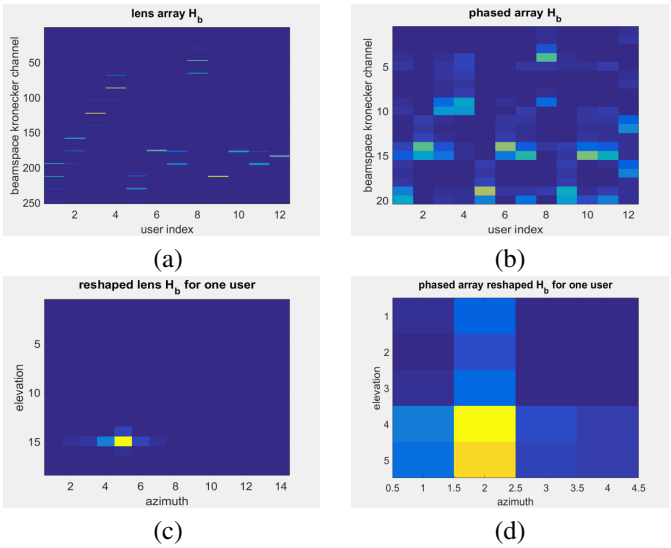


Fig. 7. Illustration of beamspace channel matrices. (a) Kronecker channel matrix for CAP-MIMO AP for 12 users. (b) Kronecker channel matrix for phased array AP for 12 users. (c) Azimuth-elevation beamspace channel matrix for one user for CAP-MIMO AP. (d) Azimuth-elevation beamspace channel matrix for one user for phased array AP.

beamdwidths in elevation and azimuth) of the CAP-MIMO AP is $N_{RF} = \sqrt{n_b} = 12$ times smaller than that of the phased array AP. This is directly related to the difference in the array gains, which is reflected in the SNR gain of CAP-MIMO AP in the idealized plots. But it also results in higher interference in the phased array AP relative to the CAP-MIMO AP. This effect is illustrated in Fig. 8 in which the idealized and actual per-user rates of the two APs are compared for: (a) MMSE receiver (interference suppression) and (b) MF receiver (no interference suppression). As evident, the loss in (actual) performance of MF receiver relative to MMSE receiver is larger for phased array AP than that for CAP-MIMO AP.

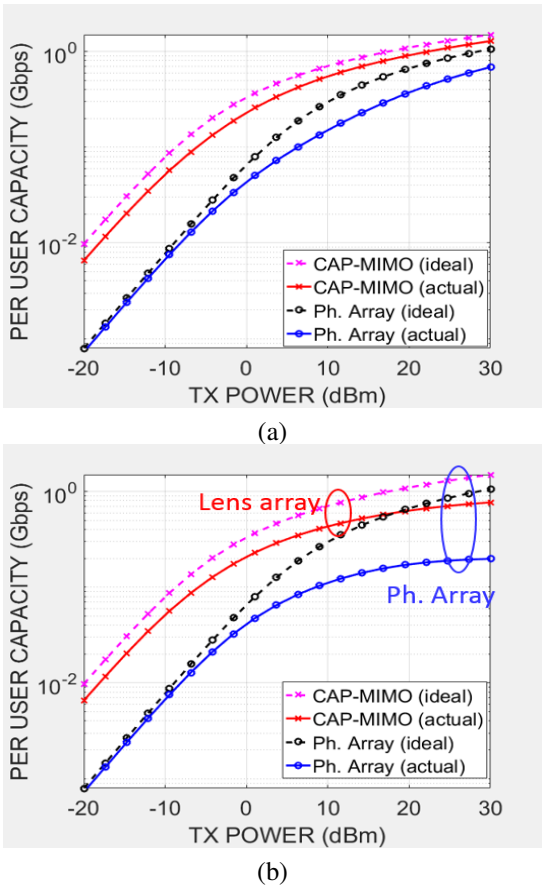


Fig. 8. Average per-user rate comparison of phased array and CAP-MIMO APs with or without interference suppression. (a) MMSE interference suppression. (b) MF processing (no interference suppression).

## REFERENCES


[1] Z. Pi and F. Khan, "An introduction to millmeter-wave mobile broadband systems," *IEEE Commununications Magazine*, pp. 101–107, June 2011.

[2] S. Rangan, T. Rappaport, and E. Erkip, "Millimeter-wave cellular wireless networks: Potentials and challenges," *Proc. IEEE*, pp. 366–385, Mar. 2014.

[3] A. L. Swindlehurst, E. Ayanoglu, P. Heydari, and F. Capolino, "Millimeter-wave massive mimo: the next wireless revolution?" *IEEE Communications Magazine*, vol. 52, no. 9, pp. 56–62, Sep. 2014.

[4] R. W. Heath, N. González-Prelcic, S. Rangan, W. Roh, and A. M. Sayeed, "An overview of signal processing techniques for millimeter wave MIMO systems," *IEEE Journal of Selected Topics in Signal Processing*, vol. 10, no. 3, pp. 436–453, April 2016.

[5] A. Sayeed and N. Behdad, "Continuous aperture phased MIMO: Basic theory and applicatons," *Proc. 2010 Annual Allerton Conference on Communications, Control and Computers*, pp. 1196–1203, Sep. 2010.

[6] J. Brady, N. Behdad, and A. Sayeed, "Beamspace MIMO for millimeter-wave communications: System architecture, modeling, analysis and measurements," *IEEE Transactions on Antenna and Propagation*, pp. 3814–3827, July 2013.

[7] P. Amadori and C. Masouros, "Low RF-Complexity Millimeter-Wave Beamspace-MIMO Systems by Beam Selection," *Communications, IEEE Transactions on*, vol. 63, no. 6, pp. 2212–2223, June 2015.

[8] X. Gao, L. Dai, and A. Sayeed, "Low RF-complexity technologies for 5G millimeter-wave MIMO systems with large antenna arrays,," *IEEE Commun. Mag. (accepted for publication)*, 2017.

[9] Y. Zeng, R. Zhang, and Z. N. Chen, "Electromagnetic lens-focusing antenna enabled massive MIMO: Performance improvement and cost reduction," *IEEE J. Sel. Areas Commun.*, vol. 32, no. 6, pp. 1194–1206, June 2016.

[10] Y. Zeng and R. Zhang, "Millimeter wave MIMO with lens antenna array: A new path division multiplexing paradigm," *IEEE Trans. Commun.*, vol. 64, no. 4, pp. 1557–1571, Apr. 2016.

[11] A. Sayeed and J. Brady, "Beamspace MIMO for high-dimensional multiuser communication at millimeter-wave frequencies," *2013 IEEE Global Communications Conference*, pp. 3785–3789, Dec. 2013.

[12] J. Brady and A. Sayeed, "Beamspace MU-MIMO for high-density gigabit small cell access at millimeter-wave frequencies," *2014 IEEE International Workshop on Signal Processing Advances for Wireless Communications*, 2014.

[13] A. M. Sayeed, "Deconstructing multi-antenna fading channels," *IEEE Trans. Signal Processing*, vol. 50, no. 10, pp. 2563–2579, Oct. 2002.

[14] A. Sayeed and J. Brady, *Millimeter-Wave MIMO Transceivers: Theory, Design and Implementation.* Signal Processing for 5G: Algorithms and Implementations (F.-L. Luo and J. Zhang, Eds.), IEEE-Wiley, 2016.

[15] J. Hogan and A. Sayeed, "Beam selection for performance-complexity optimization in high-dimensional MIMO systems," *50-th Annual Conference on Information Sciences and Systems (CISS)*, Mar. 2016.

[16] A. M. Sayeed and V. Raghavan, "Maximizing MIMO Capacity in Sparse Multipath with Reconfigurable Antenna Arrays," *IEEE J. Select. Topics in Signal Processing*, pp. 156–166, June 2007.

[17] J. W. Brewer, "Kronecker products and matrix calculus in system theory," *IEEE Trans. Circ. and Syst.*, vol. 25, no. 9, pp. 772–781, Sep. 1978.